LWT - Food Science and Technology 167 (2022) 113868

Contents lists available at ScienceDirect

LWT

journal homepage: www.elsevier.com/locate/lwt

# Study on vacuum drying kinetics and processing of the *Lonicera japonica* Thunb. aqueous extracts

Peng Xu [a,b,c], Zhentao Zhang [b,c], Xueyuan Peng [a,*], Junling Yang [b,c], Xiaoqiong Li [b,c], Tiejian Yuan [b,c,d], Xiaohan Jia [a], Yaoyang Liu [c], Olim Abdullaev [e], Janar Jenis [f]

[a] Xi'an Jiaotong University, Xi'an, Shanxi, China
[b] Technical Institute of Physics and Chemistry, Chinese Academy of Sciences, Beijing, China
[c] Key Laboratory of Equipment and Energy-saving Technology on Food & Pharmaceutical Quality Processing, Storage and Transportation, China National Light Industry, Beijing, China
[d] Qingdao University of Science and Technology, Qingdao, China
[e] Namangan State University of Uzbekistam, Namangan, Uzbekistan
[f] Research Center for Medicinal Plants, Al-Farabi Kazakh National University, Almaty, Kazakhstan

ARTICLE INFO

*Keywords:*
*L. japonica* Thunb.
Aqueous extracts
Vacuum drying
Drying kinetics
Physicochemical properties

ABSTRACT

To reveal the vacuum drying mechanism of aqueous extracts and develop vacuum drying processing to provide theoretical guidance for *Lonicera japonica* Thunb. aqueous extracts, the effects of vacuum pressure (10, 15, 20, 25, 30 kPa), drying temperature (80, 90, 100, 110, 120 °C), and material thickness (2, 4 mm) of vacuum drying on the moisture ratio, drying rate, material temperature, moisture effective diffusivity, activation energy, content and distribution of moisture, water-solubility, flowability, antioxidant capacity, and the contents of chlorogenic acid and galuteolin contents were investigated. Results showed that the drying mechanism of the aqueous extracts was different from that of conventional porous media, which contains drying stagnation and boiling phenomenon. The initial bound water content of the aqueous extracts was 100%, and the bound water will not convert to free water during vacuum drying. The best vacuum drying process for the *L. japonica* Thunb. aqueous extracts was 30 min, 4 mm, 120 °C and 10 kPa.

## 1. Introduction

*Lonicera japonica* Thunb. (Caprifoliaceae) belonging to the Caprifoliaceae family, native to eastern Asia, is known as a famous traditional Chinese medicine (Jin Yin Hua in Chinese) (Qiu et al., 2021). Pharmacological studies have demonstrated that *L. japonica* Thunb. has numerous phytochemicals and active constituents, of which chlorogenic acid and flavonoids are the standard compounds used to assess its chemical quality (Ge, Wan, Tang, Chen, Li, Zhang et al., 2018). *L. japonica* Thunb. possesses antibacterial, anti-inflammatory and is widely used for the prevention and treatment of severe acute respiratory syndromes, H1N1 influenza, fever and infections (Rahman & Chul Kang, 2009; Yang et al., 2019).

*L. japonica* extract powder, the dried product of *L. japonica* flower aqueous extracts, is a common raw material for lots of traditional Chinese medicines (TCM) preparations, such as Lianhua Qingwen granule which has potential clinical advantages for COVID-19 patients with improving clinical symptoms (Xiao et al., 2020). Drying is an indispensable step for TCM extract powder to extend the storage period and is easy to process into tablets, granules and other solid preparations (Tan, Kha, Parks, Stathopoulos, & Roach, 2015). Due to the characteristics of high viscosity, high sugar content and poor air permeability of the aqueous extracts, the conventional drying method will lead to the disadvantages of poor quality and low production efficiency. Therefore, vacuum dying has been the main drying method for sticky TCM aqueous extracts as heat is provided by conduction, which can not only shorten the drying time, but also contributes to high-quality dried products (Li, Zhang, & Yang, 2019).

It is worth noting that, in many pharmaceutical factories, the phenomenon of using one method to process kinds of TCM is serious, resulting in difficulty to guarantee the efficacy of medicines (Santhalakshmy, John, Francis, & Sabeena, 2015). At present, most of the research on the TCM raw materials and decoction pieces drying focuses on parameter optimization, but the research on the principle of the

* The corresponding author. Xi 'an Jiaotong University, 28 Xianning West Road, Xi 'an, Shaanxi Province, China.
*E-mail address:* xypeng@mail.xjtu.edu.cn (X. Peng).

https://doi.org/10.1016/j.lwt.2022.113868
Received 3 June 2022; Received in revised form 6 July 2022; Accepted 8 August 2022
Available online 11 August 2022

drying kinetics and the suitability of the aqueous extracts is relatively few, which restricting the development of the TCM products (Xu, Peng, Yuan, Yang, Li, Zhang et al., 2021). Therefore, sound knowledge of drying mechanisms and quality research of the TCM aqueous extracts is crucial to facilitate the production and clinical use of TCM (Aral & Vildan Bese, 2016).

Drying is a complex process involving heat and mass transfer, dried materials are regarded as porous media usually (Feng, Ping, Zhou, Yagoub, Xu, Sun et al., 2020). According to the phase state, motion form and driving force of moisture in the process of moisture transfer in solid materials, researchers have proposed the liquid diffusion theory, capillary theory, Luikov theory and other theories to reveal the heat and mass transfer phenomenon during drying. (Bhaskaran et al., 2022). But the aqueous extracts are high viscous fluid, which is different from conventional drying materials, its unique drying characteristics have not been revealed yet (Xu, Peng, Yuan, Yang, Li, Zhang et al., 2021). The drying kinetics can be effectively revealed by studying the effect of different drying conditions on drying rate, moisture effective diffusivity and activation energy, moreover, the content of free water and bound water in drying materials is also helpful to investigate the heat and mass transfer during drying (Chen, Dong, Li, Guo, & Wang, 2019). And as a non-destructive and fast detection technology, low-field nuclear magnetic resonance (LF-NMF) has wildly used in measuring water content, state and distribution inside dying materials (Jiang, Bai, Sun, & Zhu, 2020). The specific process can provide scientific theoretical guidance for quality assurance production, and the study of the physicochemical properties of the extract powder can effectively develop the drying process (Li et al., 2017).

Consequently, to reveal the vacuum drying mechanism of high viscous aqueous extracts and develop the vacuum processing for ensure the quality and medicinal properties of *L. japonica* Thunb. extract powder. In this paper, vacuum pressure (10, 15, 20, 25, 30 kPa), drying temperature (80, 90, 100, 110, 120 °C), and material thickness (2, 4 mm) were selected as typical influencing factors of vacuum drying, and the effects of vacuum drying on the moisture ratio, drying rate, material temperature, effective moisture diffusivity, activation energy, content of different moisture, water-solubility, flowability, antioxidant capacity, and the contents of chlorogenic acid and galuteolin contents of the *L. japonica* Thunb. aqueous extracts and extract powder were investigated.

## 2. Materials and methods

### 2.1. Preparation the aqueous extracts of L. japonica Thunb. for drying

*L. japonica* Thunb. raw materials were obtained from Jiangxi Yuxia Traditional Chinses Medicine Co. Ltd., extracted and concentrated to a density of 1.25 ± 0.01 g/cm$^3$, and the initial dry basis (d.b.) moisture content was 74.15% ± 0.02%.

### 2.2. Vacuum drying equipment

The vacuum drying equipment was designed and built by the Technical Institute of Physics and Chemistry. The schematic diagram and

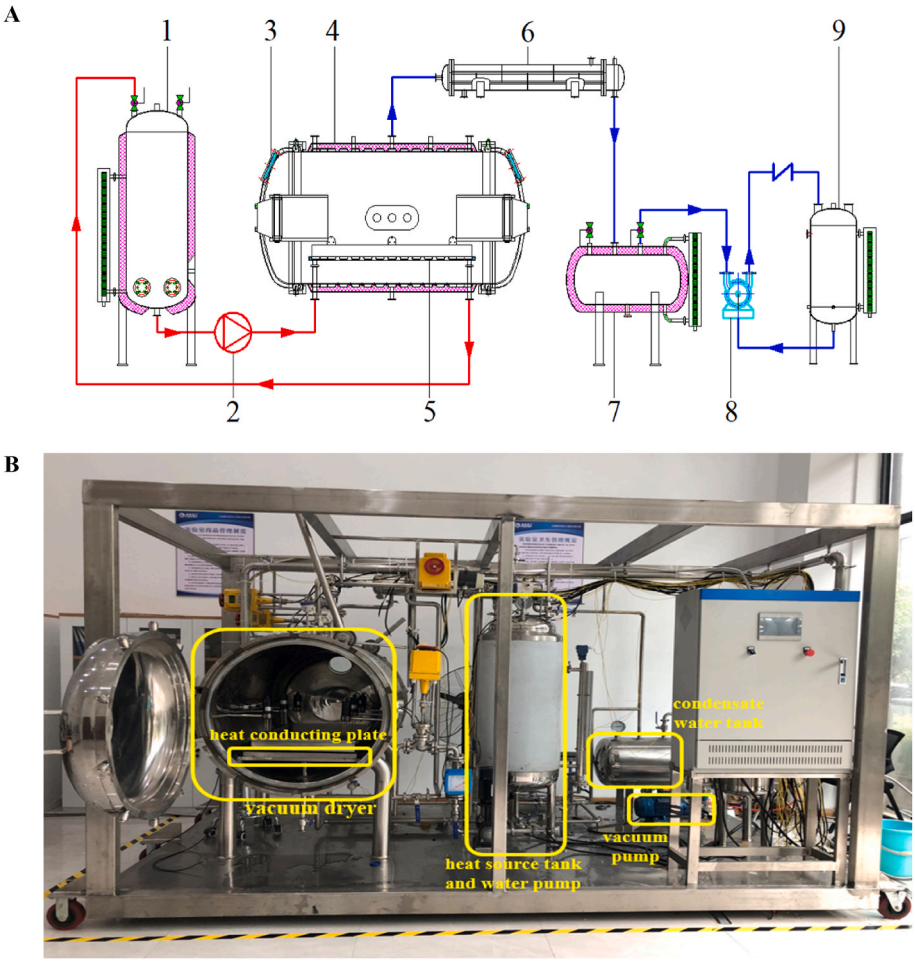


**Fig. 1.** The schematic diagram and physical picture of vacuum drying equipment. 1. Heat source tank, 2. Heat water pump, 3. Observation window, 4. Vacuum dryer, 5. Heat conducting plate, 6. Heat exchanger, 7. Condensate water tank, 8. Vacuum pump, 9. Circulating water tank.

physical picture were shown in Fig. 1. The aqueous extracts are heated by the heat-conduction plate in the vacuum dryer. The temperature of the plate was controlled by a PID controller (Omron, Model E5CN) with accuracy ± 0.1 °C. The pressure in the vacuum dryer was regulate by a vacuum pump, the vapor evaporates and condenses into liquid.

### 2.3. Experiment design

Vacuum pressure (10, 15, 20, 25, 30 kPa), drying temperature (80, 90, 100, 110, 120 °C) and material thickness (2, 4 mm) were selected to study on the vacuum drying kinetics of *L. japonica* Thunb. aqueous extracts and physicochemical properties of *L. japonica* Thunb. extract powder.

The experimental process is as follows: the aqueous extracts were poured on the heat conducting plate to 2 mm or 4 mm, closed the door and heating the water. Opening the electric valves and the vacuum pump when the heated water reached the design drying temperature. Turned on the hot water pump after the vacuum pressure reached the target value. The low pressure and drying temperature were kept stable by adjusting valves and the electric heaters. Weighed and stored dried samples every 10 min and repeated the vacuum drying experiment with same new drying materials until the moisture content is less than and close to 0.1 kg/kg (d.b.) or 10%, as determined following the AOAC method no.934.06 (AOAC, 1990). Each experiment was performed in triplicate.

After vacuum drying, crushed the dried products into powder by a grinder (FW135, Taisite instrument Co., Ltd., China), and sifted by an 80 mesh sieve (Pharmacopoeia sieve, Ejiang, Shanyn, China).

### 2.4. Drying kinetics

#### 2.4.1. Moisture ratio (MR)

The moisture ratio was calculated by the following equation:

$$MR = \frac{M_t - M_e}{M_0 - M_e} \tag{1}$$

where, $M_t$ is the moisture content at time $t$, (kg/kg), $M_0$ is the initial moisture content, (kg/kg), $M_e$ is the equilibrium moisture content, which is usually assumed to be zero. (Chao, Li, & Fan, 2022).

#### 2.4.2. Drying rate (DR)

The *DR* was calculated by formula given below:

$$DR = \frac{M_{t1} - M_{t2}}{t_2 - t_1} \tag{2}$$

where $M_{t1}$ and $M_{t2}$ are moisture content, g $H_2O$/g d.b. of *L. japonica* Thunb. aqueous extracts at drying time $t_1$ and $t_2$ (h), respectively (Hawa et al., 2021).

#### 2.4.3. Measurement of the material temperature (MT)

Three temperature sensors (accuracy of ±0.2 °C) were used to measure the material temperature during vacuum drying. The measured average temperature data was calculated as the following equation:

$$Hc = \int_{t_0}^{t_i} T_i dt \tag{3}$$

where *Hc* is the average temperature of the aqueous extracts, (°C), $t_0$ and $t_i$ are the vacuum drying time $i$, (s), $T_i$ means the temperature at the moment $i$ of the drying process, (°C) (Jiang, Xiao, et al., 2020).

#### 2.4.4. Effective moisture diffusivity ($D_{eff}$) and activation energy ($E_a$)

Fick's second law of unsteady state diffusion was employed to describe $D_{eff}$, it can be solved as the following equations:

$$\frac{\partial M}{\partial t} = \nabla\left[D_{eff}(\nabla M)\right] \tag{4}$$

$$MR = \frac{M_t - M_e}{M_0 - M_e} = \frac{8}{\pi^2}\exp\left(-\pi^2\frac{D_{eff}t}{4L^2}\right) \tag{5}$$

where, $D_{eff}$ is effective moisture diffusivity ($m^2$/s), $L$ is the half thickness of the aqueous extracts (m), $t$ is the vacuum drying time (s) (Chen et al., 2020).

According to the Arrhenius-type relationship:

$$D_{eff} = D_o \exp\left(-\frac{E_a}{RT}\right) \tag{6}$$

where, $D_o$ is the pre-exponential factor ($m^2$/s), $E_a$ is the activation energy (kJ/mol), $R$ is the gas constant (8.314J/mol K), $T$ means the absolute temperature (K). The $E_a$ was calculated by plotting the nature logarithm of $D_{eff}$ versus reciprocal of the absolute temperature (Sehrawat, Nema, & Kaur, 2018).

#### 2.4.5. NMR analysis

A LF-NMR (NMI20-025V–I, Suzhou, China, Newman Company) corresponding to a 20 MHz resonance frequency for protons was applied. Main parameters: operating temperature 25 °C, TE = 0.2 ms, TW = 4500 ms, NECH = 2000, NS = 64, PRG = 3. The transverse relaxation time (T2) was determined by the Carr Purcell Meiboom Gill (CPMG) pulse sequence. The CPMG decay curves were analyzed by multi-exponential fitting.

### 2.5. Physicochemical properties

#### 2.5.1. Water solubility

Transferred 1 g extract powder and 100 ml distilled water to a blender running 5 min at 500 rpm(R-SX, Shanghai Yanshe, China), then the solution was centrifuged 5 min at 2000 rpm (80–2, Changzhou Yitong instrument manufacturing Co., Ltd., China). 20 ml supernatant oven dried at 110 °C to a constant weight.

$$ws = \frac{w_0 - w_1}{w_0} \times 100\% \tag{7}$$

where $w_1$ is the mass of undissolved powder in suspension solution and $w_0$ is the initial mass of total powder (Chen, Chen, Meng, Wang, & Long, 2019).

#### 2.5.2. Flowability

The Hausner ratio (HR) and Carr index (CI) were used to evaluate the flowability of the *L. japonica* Thunb. extract powder (Hazlett, Schmidmeier, & O'Mahony, 2021). 20 g sample was loaded into a 100 ml graduated cylinder, the tapped density ($\rho_{tapped}$) was calculate by the measured volume from the sylinder, tapped the cylinder 200 times, and the volume of the extract powder was read to determine the tapped density ($\rho_{tapped}$).

$$CI = \frac{\rho_{tapped} - \rho_{bulk}}{\rho_{tapped}} \times 100\% \tag{8}$$

$$HR = \frac{\rho_{tapped}}{\rho_{bulk}} \tag{9}$$

#### 2.5.3. Chlorogenic acid and galuteolin contents

The chlorogenic acid and galuteolin of standards and dried extract powder were measured using HPLC (1260 Infinity II Prime, Agilent, California, US), the methodology was as follows: weighed the chlorogenic acid and galuteolin standards 0.0041 g and 0.005 g respectively, and added 75% methanol to dilute into 5 concentrations of standard solution. The concentrations of 5 standard solutions were a (0.41, 0.5

mg/mL), b (0.205, 0.25 mg/mL), c (0.164, 0.2 mg/mL), d (0.1025, 0.125 mg/mL), and e (0.082, 0.1 mg/mL).

Took 0.5 g of each extract powder samples and added 50 ml 75% methanol with ultrasound at 40 kHz, 400 W for 30 min. Then cooling and use 75% methanol to make up for the lost weight, shaken well and filtered.

A C18 column (Shimadzu, Tokyo, Japan) was used to separate the chlorogenic acid and galuteolin in a binary solvent consisting of acetonitrile ($CH_3CN$, solvent A) and 0.4% glacial acetic acid ($C_2H_2O_2$, solvent B) with a gradient elution: 0–15 min, 10% of solvent A, 90% of solvent B; 15–30 min, 20% A and 80% B; 30–40 min, 30% A and 70% B. The wavelength was 350 nm, and the flow rate was 1.0 mL/min.

### 2.5.4. Antioxidant capacity (AC)

The AC of the *L. japonica* Thunb. extract powder was evaluated by the DPPH (2,2-Diphenyl-1-picrylhydrazyl) free radical scavenging test (Sridhar & Linton, 2019). 0.1 mL diluted sample was mixed with 3.9 mL DPPH ethanolic solution (0.024 g/L), followed by dark incubation at 37 °C for 30 min. The absorbance was measured (514 nm) by a UV spectrophotometer (UV-2450, Shimadzu, Japan). And the DPPH was calculated by following:

$$\text{inhibition}\% = \frac{(A_0 - A_1)}{A_1} \times 100\% \quad (10)$$

where $A_0$ and $A_1$ are the absorbance of the blank solvent control and the text sample respectively.

The DPPH inhibition percent values of samples were plotted to a standard curve of ethanolic solution of Trolox ($R^2 = 0.9958$) which ranging from 10 to 100 mg/L. The results were expressed as μmol of Trolox equivalent/g of dried powder.

## 2.6. Statistical analysis

All analyses were done in triplicate. The data were analyzed by SPSS statistics software (Version 21.0, SPSS Inc., Chicago, IL, USA). The statistical analysis was performed with Origin (Version 2022; Origin-Lab, Northampton, Massachusetts, USA).

## 3. Results and discussion

### 3.1. Drying kinetics

The variations of *MR* versus drying time are presented in Fig. 2. The final dry basis moisture content of the *L. japonica* Thunb. extract powder is required less than 10% in the *Pharmacopoeia*, that is, the *MR* should be less than 0.135. When the material thickness is 2 or 4 mm, the corresponding drying time is 10–40 min or 30–50 min respectively. It would be taken less time to drying when the material thickness is 2 mm. And the higher the drying temperature or the lower the vacuum pressure, the shorter the drying time.

The above results can be interpreted that, the aqueous extracts are high viscous fluid, when the superheat (it means the difference between drying temperature and saturated vapor temperature) is high enough, it boils during vacuum drying (Tanaka, Miyazaki, & Yabuki, 2020). The saturated vapor temperature will decrease when the pressure of the drying environment is less than the atmospheric pressure. When the drying temperature is higher or the vacuum pressure is lower, the superheat become greater, and the more obvious the boiling phenomenon. Under the action of large pressure difference and bubbles disturbance, the heat and mass transfer rate are improved, and drying time is shortened (Lao, Zhang, Sakamon, & Ye, 2019).

Notably, a rare phenomenon is found under some vacuum drying conditions in the figures of *MR* versus drying time, when the aqueous extracts are dried to a certain *MR*, it will not significantly decrease with drying time increases, and it cannot be finally dried into powder (the

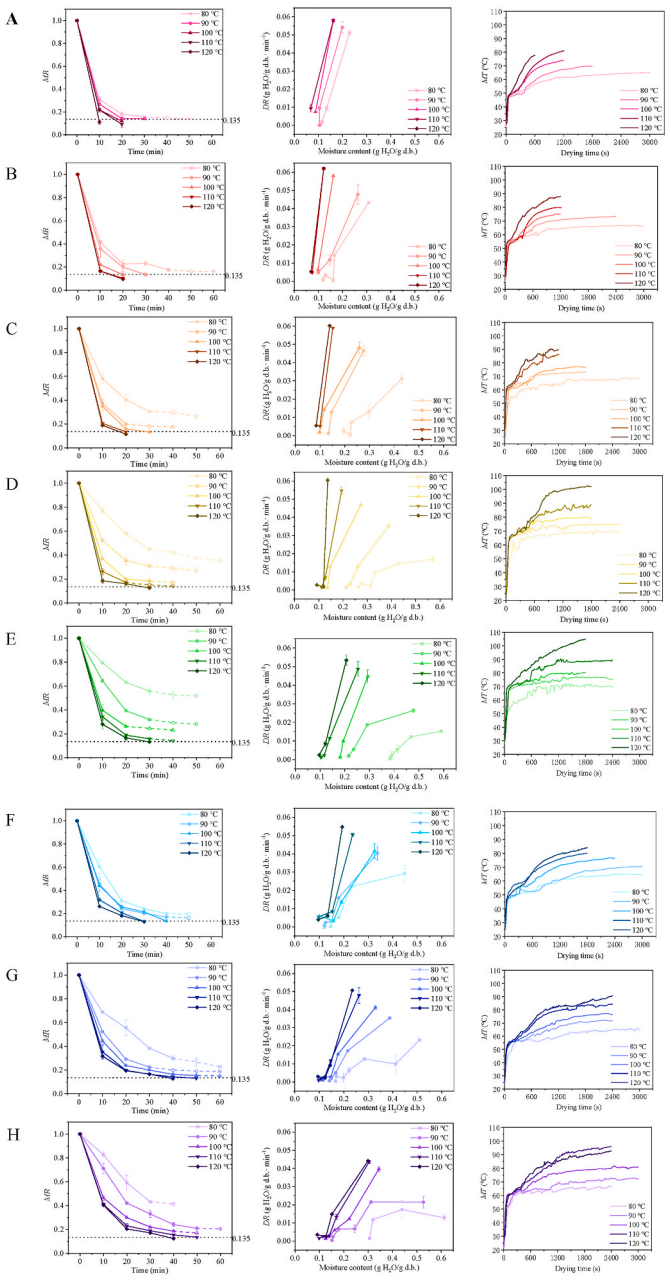


**Fig. 2.** Effect of vacuum pressure, drying temperature and thickness on the change of Moisture ratio (*MR*), Drying rate (*DR*), and Material temperature (*MT*) of the aqueous extracts during vacuum drying. A: 2 mm, 10 kPa; B: 2 mm, 15 kPa; C: 2 mm, 20 kPa; D: 2 mm, 25 kPa; E: 2 mm, 30 kPa; F: 4 mm, 10 kPa; J: 4 mm, 15 kPa; H: 4 mm, 20 kPa. Different values are shown as significantly different ($p < 0.05$).

physical states present in Fig. 3. C, D, I). For example, when the material thickness is 2 mm, the vacuum pressure is 25 kPa, and the drying temperature is 80 and 90 °C, the *MR* are reduced to 0.35 and 0.27 and almost unchanged when the drying time is more than 30 min. This phenomenon is more obvious of 4 mm material thickness, but it does not occur in solid materials vacuum drying. This may be because the drying activation energy of the aqueous extracts is much higher than that of porous media. The drying activation energy is an energy threshold that the water molecules inside the material must reach before removal (Asif & Shi, 2004). With the moisture content decrease, the viscosity increases gradually, the binding force between water and macromolecules of TCM also increases, and there is not enough activation energy to make the

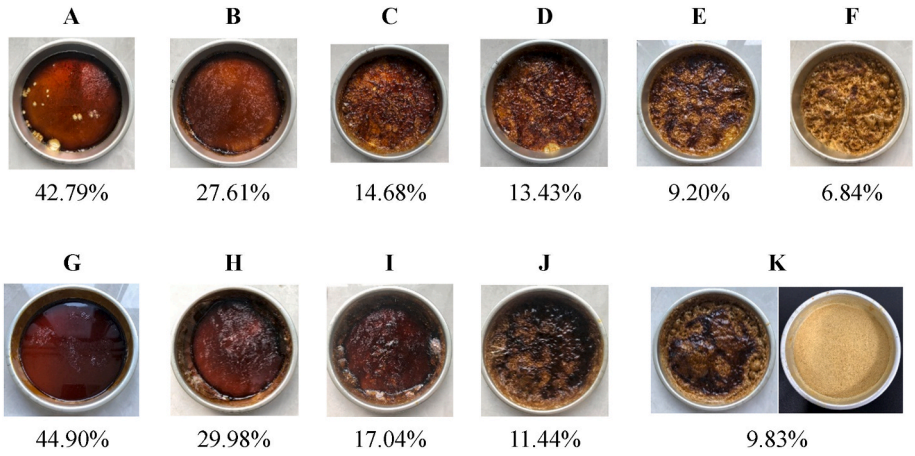


**Fig. 3.** The physical picture and moisture ratio (dry basis) of the aqueous extracts after vacuum drying. A: 2 mm, 25 kPa, 80 °C, 20 min; B: 2 mm, 20 kPa, 90 °C, 10 min; C: 2 mm, 20 kPa, 90 °C, 20 min; D: 2 mm, 20 kPa, 90 °C, 30 min; E: 2 mm, 25 kPa, 120 °C, 30 min; F: 2 mm, 10 kPa, 110 °C, 20 min; J: 4 mm, 10 kPa, 80 °C, 10 min; H: 4 mm, 20 kPa, 120 °C, 10 min; I: 4 mm, 20 kPa, 110 °C, 20 min; J: 4 mm, 15 kPa, 100 °C, 50 min; K: 4 mm, 10 kPa, 110 °C, 30 min.

bound water escape from the aqueous extracts under low superheat conditions. It was also found through tests that when the material thickness is 2 mm and the vacuum pressure is greater than 30 kPa, or 4 mm and greater 20 kPa, the drying stagnation phenomenon will occur significantly when the drying temperature is lower than 120 °C.

The *DR* versus moisture content and *MT* versus drying time are also present in Fig. 2. The drying period in a plot graphing *DR* versus moisture content is normally divided into three distinct periods, including the initial transient period, constant rate period and falling rate period (Caccavale, De, & Ruocco, 2016). The aqueous extracts vacuum drying can also be divided into three distinct periods but with some differences. The temperature of the aqueous extracts heats up during the initial transient. At the constant rate period, the drying mechanism is different from that of porous media, that is, the water of the aqueous extracts evaporates and escapes from the materials in the form of bubbles rather than forming a water film on the surface of porous media. The superheat determines whether the aqueous extracts vacuum drying is in bubble core boiling (present in Fig. 3. A, G) or excessive boiling (present in Fig. 3. B, H), and the heat transfer coefficient and mass transfer efficiency of the two stages are different. In the falling rate period, with the loss of moisture, the solid phase of the aqueous extracts (turbid particles and macromolecules) connects, and the aqueous extracts gradually become porous media, and the remaining bound water also diffuses outward through the form of water film on the material surface (present in Fig. 3. E, J).

Fig. 2 shows that the *DR* versus moisture content ranges from 0 to 0.06 g $H_2O$/g d.b.·$min^{-1}$ and *MT* versus drying time ranges from 25 to 105 °C. The *DR* and *MT* will be higher with the higher drying temperature. When the drying temperature is the same, the *MT* will increase with the increase of vacuum pressure, because the temperature of the aqueous extracts is determined by the temperature of saturated vapor. What's more, when the material thickness is 2 mm and the drying temperature is 110 and 120 °C, the drying period only divided into constant rate period and falling rate period. Due to the superheat is relatively large under this drying condition, and the aqueous extracts are in the excessive boiling state, a large number of bubbles produce disturbances at this stage, so as to strengthen the temperature transfer, the *MT* heats up rapidly and large moisture escapes as bubbles simultaneously. However, these three periods can be seen clearly when the drying temperature is less than 100 °C.

### 3.2. Moisture effective diffusivity and activation energy

The $D_{eff}$ values of the *L. japonica* Thunb. aqueous extracts that can be dried into powders are shown in Table 1. The $D_{eff}$ of 2 mm aqueous extracts during vacuum drying ranges from $0.406 \times 10^{-9}$ to$1.350 \times 10^{-9}$ $m^2$/s, and those of 4 mm ranges from $0.970 \times 10^{-9}$ to$1.660 \times 10^{-9}$ $m^2$/s. The $D_{eff}$ of 4 mm aqueous extracts vacuum drying is bigger than that of 2 mm. The reason may be that the thicker the material, the more

**Table 1**
Effective diffusivity and Physicochemical properties of *Lonicera japonica* Thunb. extract powder samples after vacuum drying.

| No. | Vacuum drying conditions | $D_{eff}$ ($*10^{-9}$ $m^2$/s) | *ws* (%) | CI (%) | HR | AC (%) |
|---|---|---|---|---|---|---|
| 1 | 2 mm, 10 kPa, 100 °C | 0.652 | 83.2 ± 0.7$^{c}$ | 16.1 ± 0.2$^{c}$ | 1.10 ± 0.02$^{b}$ | 51.00 ± 3.6$^{c}$ |
| 2 | 2 mm, 10 kPa, 110 °C | 0.736 | 80.9 ± 0.1$^{c}$ | 20.6 ± 0.4$^{a}$ | 1.26 ± 0.02$^{a}$ | 52.77 ± 1.9$^{c}$ |
| 3 | 2 mm, 10 kPa, 120 °C | 1.350 | 82.9 ± 0.1$^{c}$ | 20.6 ± 0.3$^{a}$ | 1.26 ± 0.04$^{a}$ | 55.18 ± 2.7$^{c}$ |
| 4 | 2 mm, 15 kPa, 90 °C | 0.406 | 74.1 ± 0.2$^{e}$ | 20.6 ± 0.2$^{a}$ | 1.26 ± 0.01$^{a}$ | 33.64 ± 0.6$^{e}$ |
| 5 | 2 mm, 15 kPa, 100 °C | 0.611 | 82.1 ± 0.4$^{c}$ | 10.3 ± 0.2$^{e}$ | 1.12 ± 0.03$^{b}$ | 42.44 ± 2.7$^{d}$ |
| 6 | 2 mm, 15 kPa, 110 °C | 0.704 | 81.4 ± 0.1$^{c}$ | 16.1 ± 0.1$^{c}$ | 1.19 ± 0.04$^{b}$ | 41.97 ± 2.4$^{d}$ |
| 7 | 2 mm, 15 kPa, 120 °C | 0.729 | 79.4 ± 0.2$^{d}$ | 12.9 ± 0.1$^{e}$ | 1.15 ± 0.02$^{b}$ | 47.39 ± 3.5$^{d}$ |
| 8 | 2 mm, 20 kPa, 100 °C | 0.409 | 83.0 ± 0.2$^{c}$ | 16.1 ± 0.5$^{c}$ | 1.19 ± 0.05$^{b}$ | 43.73 ± 1.7$^{d}$ |
| 9 | 2 mm, 20 kPa, 110 °C | 0.606 | 82.4 ± 0.1$^{c}$ | 17.6 ± 0.3$^{c}$ | 1.21 ± 0.0.6$^{a}$ | 38.78 ± 2.1$^{e}$ |
| 10 | 2 mm, 20 kPa, 120 °C | 0.663 | 78.4 ± 0.1$^{d}$ | 21.9 ± 0.2$^{a}$ | 1.28 ± 0.01$^{a}$ | 51.42 ± 3.0$^{c}$ |
| 11 | 2 mm, 25 kPa, 120 °C | 0.423 | 83.3 ± 0.2$^{c}$ | 14.2 ± 0.4$^{d}$ | 1.17 ± 0.03$^{b}$ | 53.32 ± 2.1$^{c}$ |
| 12 | 2 mm, 30 kPa, 120 °C | 0.411 | 80.0 ± 0.1$^{c}$ | 16.7 ± 0.1$^{c}$ | 1.20 ± 0.04$^{a}$ | 51.91 ± 1.1$^{c}$ |
| 13 | 4 mm, 10 kPa, 100 °C | 1.210 | 82.4 ± 0.2$^{c}$ | 17.9 ± 0.3$^{c}$ | 1.22 ± 0.03$^{a}$ | 37.21 ± 1.8$^{e}$ |
| 14 | 4 mm, 10 kPa, 110 °C | 1.630 | 82.7 ± 0.2$^{c}$ | 16.1 ± 0.1$^{c}$ | 1.19 ± 0.03$^{b}$ | 59.24 ± 1.8$^{b}$ |
| 15 | 4 mm, 10 kPa, 120 °C | 1.660 | 81.9 ± 0.2$^{c}$ | 18.2 ± 0.1$^{b}$ | 1.26 ± 0.04$^{a}$ | 70.95 ± 2.2$^{a}$ |
| 16 | 4 mm, 15 kPa, 110 °C | 0.986 | 87.4 ± 0.3$^{d}$ | 18.2 ± 0.4$^{b}$ | 1.22 ± 0.03$^{a}$ | 50.92 ± 3.6$^{c}$ |
| 17 | 4 mm, 15 kPa, 120 °C | 1.250 | 82.2 ± 0.1$^{a}$ | 17.6 ± 0.3$^{c}$ | 1.21 ± 0.04$^{a}$ | 55.64 ± 2.3$^{c}$ |
| 18 | 4 mm, 20 kPa, 110 °C | 0.970 | 86.0 ± 0.2$^{b}$ | 18.8 ± 0.2$^{b}$ | 1.23 ± 0.01$^{a}$ | 39.38 ± 3.2$^{e}$ |
| 19 | 4 mm, 20 kPa, 120 °C | 1.270 | 86.3 ± 0.2$^{b}$ | 19.4 ± 0.2$^{b}$ | 1.24 ± 0.03$^{a}$ | 61.11 ± 2.0$^{b}$ |

Different values are shown as significantly different ($p < 0.05$).

moisture passes through the dried product per unit time during vacuum drying. In addition, the $D_{eff}$ values increase with the vacuum pressure decreases or drying temperature increases, which is fully confirmed the previous drying kinetics and other studies (Azeez, Adebisi, Oyedeji, Adetoro, & Tijani, 2019).

Compared with the $D_{eff}$ values previously reported, it was found that, the $D_{eff}$ of the aqueous extracts undergoing vacuum drying was much bigger than that of conventional porous media, such as apple, banana, pear, carrot, potato (Khan, Kumar, Joardder, & Karim, 2016), bitter orange (Xu, Peng, Yang, Li, Zhang, Jia et al., 2021) and wolfberry (Zhao, Wei, Hao, Han, Ding, & Yang et al., 2019). There are two main reasons, in the first place, the diffusion of moisture in solids generally takes place in the falling rate period, it is a complex process composed of molecular diffusion, capillary flow and surface diffusion (Mbegbu, Nwajinka, & Amaefule, 2021), capillary flow means a part of moisture inside the porous media is transferred through the capillary microchannels. The aqueous extracts also could be regarded as porous media in the falling rate period, however, the channels, that can be seen by electron microscopy, are much larger than that of the capillary microchannels (Xu, Peng, Yuan, Yang, Li, & Zhang et al., 2021), the moisture could be diffused at a higher rate. In the second place, most of the water discharged from porous media is bound water in the falling rate period, the bound water of typical drying materials exists in plant cells, whereas the bound water of the aqueous extracts is water on polar groups on the surface of sugars and macromolecules. It can escape from the surface more easily than inside the plant cells when the activation energy is sufficient.

The $D_{eff}$ shown in Fig. 4 (the case of drying stagnation is not considered, it greatly affects the results of the $D_{eff}$ values), For 2 mm aqueous extracts, the $E_a$ values are 322.3, 367.4, 402.4, 596.3, 597.2 kJ/mol when the vacuum pressure is 10, 15, 20, 25, 30 kPa, respectively, and for 4 mm, the $E_a$ values are 266.3, 332.9, 389.4 kJ/mol when the vacuum pressure is 10, 15, 20 kPa. The ranges of these values are much larger than those of porous media previously studied, such as bitter orange (Xu, Peng, Yang, Li, Zhang, Jia et al., 2021) and elephant cassava (Kosasih, Zikri, & Dzaky, 2020). $D_{eff}$ was mainly dependent on drying conditions and the physicochemical properties of the products, such as their composition, thickness, cultivar, and ripening stage (Deng, Xiong, Sutat, Mujumdar, Pet, Yang et al., 2022). It confirms the previous explanation for the moisture stagnation. The higher the vacuum pressure, the greater the $D_{eff}$ value. This means that drying becomes more difficult under higher vacuum pressure. That is exactly for the same reason as the previous drying kinetics of the aqueous extracts.

### 3.3. The moisture status

The relaxation time (T2) inversion spectra curves were present in Fig. 5., which is closely related to water state and the chemical environment of protons (Yang, Han, Xia, Xu, & Wu, 2021). The dimensionless integral area of NMR is the number of hydrogen protons in the drying sample. Therefore, the integrated area covered by the peaks of curves is the content of the corresponding state moisture, and the total integral area represents the total water content in the sample (Sun, Zhang, & Yang, 2019). The peak less than 10 ms is bound water, which is the water bind tightly to large molecules such as sugars and proteins. The other two peaks (0–100 ms and 100–1000 ms) are immobilized water and free water. The moisture inside the raw aqueous extracts is 100% bound water. The bound water decreases gradually and will not transfer into free water during vacuum drying. However, the results are different from solid dry materials, such as carrot (Wang, Karim, Vidyarthi, Xie, Liu et al., 2021), blueberry (Liu, Xie, Zielinska, Pan, Wang, Deng et al., 2021) and kiwifruit (Wang, Li, Wang, Vidyarthi, Wang, Zhang et al., 2022), which has bound water, immobile water and free water, and the bound water would transfer free water during drying. Besides, also as a viscous fluid material, the initial bound water of honey is 95%, and it will also be converted into free water during vacuum drying (Jiang, Bai, et al., 2020). The reason is that honey is made of fructose and glucose, while the extract is more complex, including cellulose, hemicellulose, mucinous and a variety of polysaccharides, which bind better with water.

### 3.4. Water solubility

As shown in Table 1, there are no significant differences among the solubility of extract powders obtained at different vacuum drying conditions, similar to previously published studies (Michalska, Wojdylo, Lech, Lysiak, & Figiel, 2016). However, the thickness of the aqueous extract has a significant effect on the water solubility ($P < 0.05$). Extract powder has a higher degree of solubility with thickness increases. It can be concluded that the number of molecules increases with thickness increases, and more molecules are easy to agglomerate during vacuum drying, and decline in solubility (Mahdi Jafari, Ghalegi Ghalenoei, & Dehnad, 2017; Michalska, Wojdylo, Lech, Lysiak, & Figiel, 2016).

### 3.5. Flowability

Flowability of extract powder is an important index for mixing, capsule filling, tableting and packing for pharmaceutical applications (Hazlett et al., 2021). According to the CI and HR, the powder flowability is usually classified as 5 levels (very good, good, fair, bad, very bad), and the powder cohesiveness is classified as 3 levels (low, intermediate high), and a high HR means more cohesiveness and lower free flow capacity of powder (Santhalakshmy, John, Francis, & Sabeena, 2015). As can be seen from Table 1, most of the extract powder samples have similar and good flowability according to CI values, and most of them have small difference and are estimated to be intermediate. Moreover, material thickness, drying temperature and vacuum drying have no significant effect on the extract powder flowability, the moisture content difference between powder samples is small. It was reported that flowability is negatively correlated with the moisture content, because high moisture content can increase the cohesion between powder particles (Iqbal & Fitzpatrick, 2006).

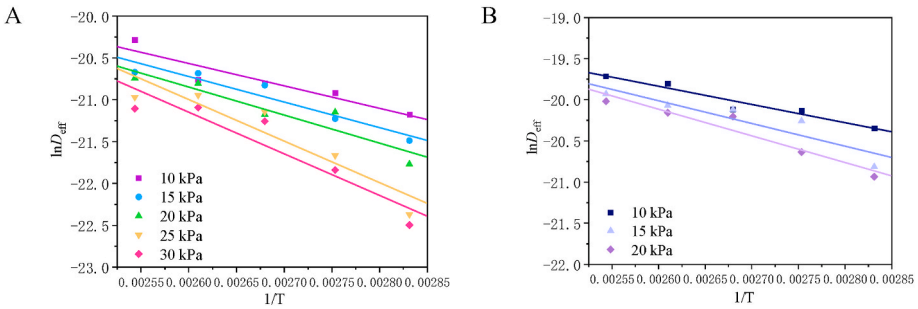


**Fig. 4.** Arrhenius-type relationship between the effective diffusivity and absolute temperature. A: material thickness is 2 mm; B: material thickness is 4 mm.

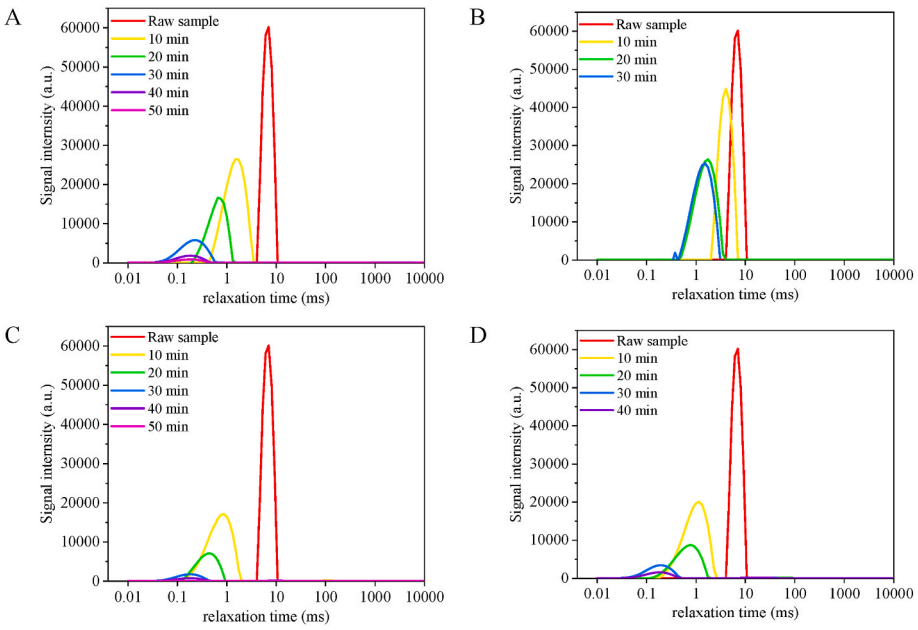


**Fig. 5.** The water state of the aqueous extracts at different vacuum drying periods. A: 2 mm, 15 kPa, 80 °C; B: 2 mm, 25 kPa, 80 °C; C: 4 mm, 10 kPa, 90 °C; D: 4 mm, 15 kPa, 90 °C.

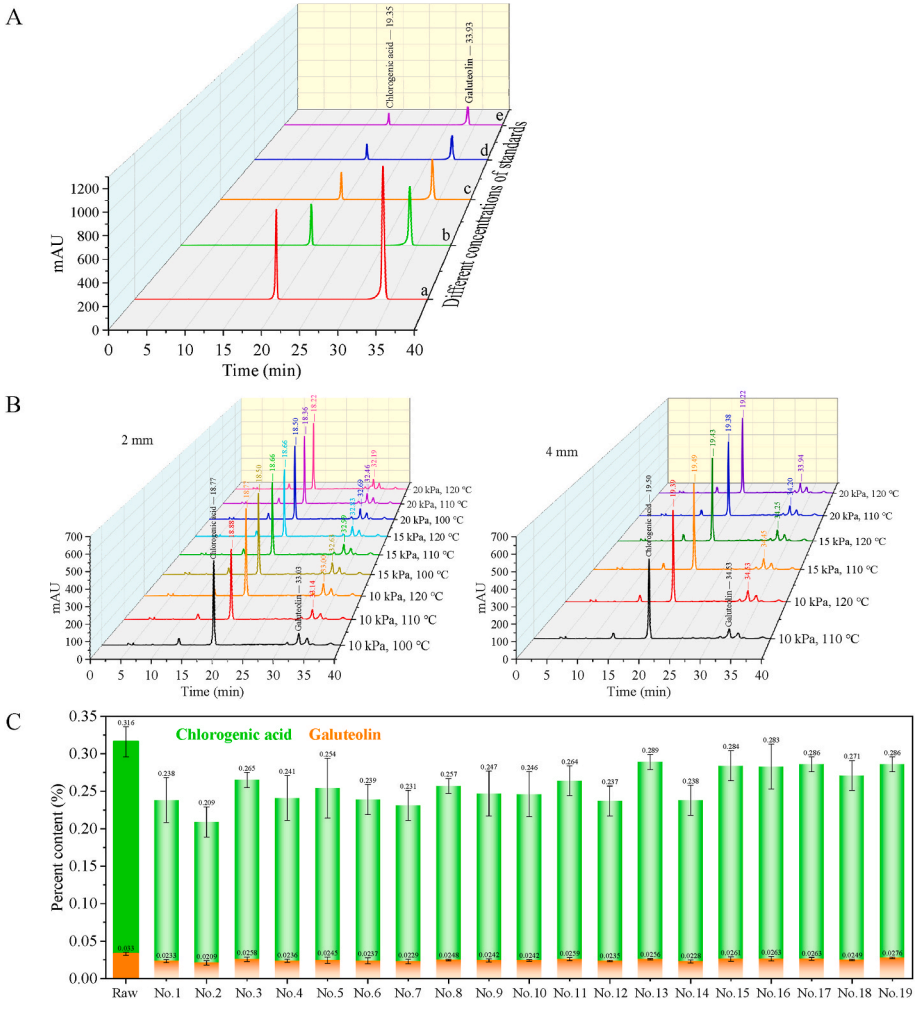


**Fig. 6.** The high-performance liquid chromatography chromatograms and the percent content of chlorogenic acid and galuteolin of *Lonicera japonica* Thunb. aqueous extracts. A: The concentrations of 5 standard solutions. a: (0.41, 0.5 mg/mL); b: (0.205, 0.25 mg/mL); c: (0.164, 0.2 mg/mL); d: (0.1025, 0.125 mg/mL); e: (0.082, 0.1 mg/mL). B: The high-performance liquid chromatography chromatograms of extract powder. C: The percent content of chlorogenic acid and galuteolin. No.1: 2 mm, 10 kPa, 100 °C; No.2: 2 mm, 10 kPa, 110 °C; No.3: 2 mm, 10 kPa, 120 °C; No.4: 2 mm, 15 kPa, 90 °C; No.5: 2 mm, 15 kPa, 100 °C; No.6: 2 mm, 15 kPa, 110 °C; No.7: 2 mm, 15 kPa, 120 °C; No.8: 2 mm, 20 kPa, 100 °C; No.9: 2 mm, 20 kPa, 110 °C; No.10: 2 mm, 20 kPa, 120 °C; No.11: 2 mm, 25 kPa, 120 °C; No.12: 2 mm, 30 kPa, 120 °C; No.13: 4 mm, 10 kPa, 100 °C; No.14: 4 mm, 10 kPa, 110 °C; No.15: 4 mm, 10 kPa, 120 °C; No.16: 4 mm, 15 kPa, 110 °C; No.17: 4 mm, 15 kPa, 120 °C; No.18: 4 mm, 20 kPa, 110 °C; No.19: 4 mm, 20 kPa, 120 °C; Different values are shown as significantly different ($p < 0.05$).

### 3.6. Chlorogenic acid and galuteolin contents

According to the HPLC chromatograms of chlorogenic acid and galuteolin of the standard samples and dried samples in Fig. 6 (A, B). The peak retention time of chlorogenic acid and flavonoids are 19.35 and 33.93 min respectively. Linear regression analysis is performed with concentration as abscissa (X) and peak area as ordinate (Y). The regression equation of chlorogenic acid is: $Y = 3.065 \times 10^7X$, $r = 0.9998$. The regression equation of galuteolin is: $Y = 6.139 \times 10^7X$, $r = 0.9998$.

The percent contents of chlorogenic acid and galuteolin of different extract powder samples are shown in Fig. 6 (C). The chlorogenic acid, as the main active ingredient of *L. japonica* Thunb. extract powder, the percent content of raw material is 0.316%, and it the ranges from 0.209% to 0.284% after vacuum drying. The galuteolin content of raw material is 0.033%, and it ranges from 0.0209% to 0.0276% of different dried powder, the content difference is small. The maximum percent content of chlorogenic acid is 0.286%, which is reduced 0.027% by compared with raw material, and the corresponding final *MT* and drying time are 73 °C, 40 min, and 83 °C, 30 min respectively. Results show that vacuum drying can effectively retain the chlorogenic acid and galuteolin content of *L. japonica* Thunb. aqueous extracts, whereas the thermal process will also make the contents loss, which depends on the magnitude and duration, and previous studies also revealed that (Hao, Wu, Li, Zhang, & Gu, 2018).

### 3.7. Antioxidant capacity

The *AC* of the *L. japonica* Thunb. extract powder is shown in Table 1, The *AC* r ranges from 39% to 79%. When the thickness and drying temperature are kept constant, the *AC* is higher when the vacuum pressure is 10.0 kPa. Previous studies have indicated that *AC* depends on vacuum drying time, because the relatively long drying time might cause the decrease and structural change of antioxidant compounds (Vega-Gálvez, Ah-Hen, Chacana, Vergara, Martínez-Monzó, García-Segovia et al., 2012). According to the previous vacuum drying kinetics, the drying time will be shorter with lower vacuum pressure. In addition, studies also showed that TCM have a stronger *AC* with higher flavonoid content (Ming & Yin, 2013).

According to the previous vacuum drying characteristics and physicochemical properties of the *L. japonica* Thunb. extract powder, the best vacuum drying condition is the drying time of 30 min, the material thickness of 4 mm, the drying temperature of 120 °C, and the vacuum pressure of 10 kPa, it results in the highest $D_{\text{eff}}$ and *AC*, i.e., $1.660 \times 10^{-9}$ $m^2/s$ and 70.95%, and higher flowability and contents of chlorogenic acid and galuteolin, i.e., 1.26, 0.284%, 0.0261%.

## 4. Conclusions

To reveal the vacuum drying mechanism of high viscous aqueous extracts and develop the vacuum processing of *L. japonica* Thunb. extract powder for ensure the quality and medicinal properties. The effects of the vacuum pressure, drying temperature, and material thickness on the vacuum drying kinetics and physicochemical property of the *L. japonica Thunb.* aqueous extracts were investigated. Results showed that the vacuum drying mechanism of aqueous extracts is different from that of porous media, it contains two characteristics: a drying stagnation phenomenon will occur when the difference between drying temperature and saturated vapor temperature is too low, the moisture of the aqueous extracts escapes to the environment in the form of boiling. Additionally, the $D_{\text{eff}}$ and $E_a$ are generally greater than those of conventional materials. The initial bound water content of the aqueous extracts is 100% and it will not transfer into free water during vacuum drying. The best vacuum drying process for the *L. japonica* Thunb. aqueous extracts is the drying time of 30 min, the vacuum pressure of 10 kPa, the drying temperature of 120 °C and the thickness of 4 mm, it results in the highest antioxidant capacity, i.e., 70.95%, and higher flowability and contents of chlorogenic acid and galuteolin, i.e., 1.26, 0.284%, 0.0261%.

## Declaration of competing interest

The authors declare that they have no known competing financial interests or personal relationships that could have appeared to influence the work reported to this paper.

## CRediT authorship contribution statement

**Peng Xu:** Conceptualization, Methodology, Software, Validation, Formal analysis, Investigation, Writing – original draft, Visualization. **Zhentao Zhang:** Resources, Supervision, Project administration, Funding acquisition. **Xueyuan Peng:** Supervision, Funding acquisition. **Junling Yang:** Resources, Writing – review & editing. **Xiaoqiong Li:** Writing – review & editing. **Tiejian Yuan:** Validation, Investigation, Writing – original draft. **Xiaohan Jia:** Supervision. **Yaoyang Liu:** Software, Investigation. **Olim Abdullaev:** Supervision. **Janar Jenis:** Supervision.

## Acknowledgements

This research was supported by the National Key Research and Developments Program of China (2021YFD1000103), the National Key Research and Development Program of Ningxia Province (2021BEG03109), the SCO scientific and technological partnership program (2020E01048).

## References

Aral, S., & Vildan Bese, A. (2016). Convective Drying of Hawthorn Fruit (Crataegus Spp.): Effect of experimental parameters on drying kinetics, color, shrinkage, and rehydration capacity. *Food Chemistry, 210*, 577–584.

Asif, A., & Shi, W. (2004). UV curable waterborne polyurethane acrylate dispersions based on hyperbranched aliphatic polyester: Effect of molecular structure on physical and thermal properties. *Polymers for Advanced Technologies, 15*(11), 669–675.

Azeez, L., Adebisi, S. A., Oyedeji, A. O., Adetoro, R. O., & Tijani, K. O. (2019). Bioactive compounds' contents, drying kinetics and mathematical modelling of tomato slices influenced by drying temperatures and time. *Journal of the Saudi Society of Agricultural Sciences, 18*(2), 120–126.

Bhaskaran, S., Pandey, D., Panda, D., Paliwal, S., Vorhauer, N., Tsotsas, E., et al. (2022). Study on film effects during isothermal drying of square capillary tube using Lattice Boltzmann method. *Drying Technology, 40*(4), 735–747.

Caccavale, P., De Bonis, M. V., & Ruocco, G. (2016). Conjugate heat and mass transfer in drying: A modeling review. *Journal of Food Engineering, 176*, 28–35.

Chao, E., Li, J., & Fan, L. (2022). Enhancing drying efficiency and quality of seed-used pumpkin using ultrasound, freeze-thawing and blanching pretreatments. *Food Chemistry, 384*, Article 132496.

Chen, J., Chen, F., Meng, Y., Wang, S., & Long, Z. (2019). Oxidized microcrystalline cellulose improve thermoplastic starch-based composite films: Thermal, mechanical and water-solubility properties. *Polymer, 168*, 228–235.

Chen, Y., Dong, H., Li, J., Guo, L., & Wang, X. (2019). Evaluation of a nondestructive NMR and MRI method for monitoring the drying process of *Gastrodia elata* Blume. *Molecules, 24*(2), 236.

Chen, Y., Li, M., Dharmasiri, T. S. K., Song, X., Liu, F., & Wang, X. (2020). Novel ultrasonic-assisted vacuum drying technique for dehydrating garlic slices and predicting the quality properties by low field nuclear magnetic resonance. *Food Chemistry, 306*, Article 125625.

Deng, L. Z., Xiong, C. H., Sutar, P. P., Mujumdar, A. S., Pei, Y. P., Yang, X. H., et al. (2022). An emerging pretreatment technology for reducing postharvest loss of vegetables-a case study of red pepper (Capsicum annuum L.) drying. *Drying Technology*, 1–9.

Feng, Y., Ping Tan, C., Zhou, C., Yagoub, A. E. A., Xu, B., Sun, Y., et al. (2020). Effect of freeze-thaw cycles pretreatment on the vacuum freeze-drying process and physicochemical properties of the dried garlic slices. *Food Chemistry, 324*, Article 126883.

Ge, L., Wan, H., Tang, S., Chen, H., Li, J., Zhang, K., et al. (2018). Novel caffeoylquinic acid derivatives from Lonicera japonica Thunb. flower buds exert pronounced anti-HBV activities. *RSC Advances, 8*(62), 35374–35385.

Hao, J., Wu, Z., Li, W., Zhang, Z., & Gu, J. (2018). A new PAT application: Optimization of processing methods for honeysuckle flower (Lonicerae Japonicae Flos) and wild honeysuckle flower (*Lonicerae* Flos). *Journal of Traditional Chinese Medical Sciences, 5*(2), 199–205.

Hawa, L. C., Ubaidillah, U., Mardiyani, S. A., Laily, A. N., Yosika, N. I. W., & Afifah, F. N. (2021). Drying kinetics of cabya (Piper retrofractum Vahl) fruit as affected by hot

water blanching under indirect forced convection solar dryer. *Solar Energy, 214*, 588–598.
Hazlett, R., Schmidmeier, C., & O'Mahony, J. A. (2021). Approaches for improving the flowability of high-protein dairy powders post spray drying – a review. *Powder Technology, 388*, 26–40.
Iqbal, T., & Fitzpatrick, J. J. (2006). Effect of storage conditions on the wall friction characteristics of three food powders. *Journal of Food Engineering, 72*(3), 273–280.
Jiang, M., Bai, X., Sun, J., & Zhu, W. (2020). Implication of ultrasonic powder and frequency for the ultrasonic vacuum drying of honey. *Drying Technology, 39*(10), 1389–1400.
Jiang, D. L., Xiao, H. W., Magdalena, Z., Zhu, G. F., Bai, T. Y., & Zheng, Z. A. (2020). Effect of pulsed vacuum drying on drying kinetics and quality of roots of *Panax Notoginseng* (Burk.) F. H. Chen (Araliaceae). *Drying Technology, 39*(16), 2234–2251.
Khan, M. I. H., Kumar, C., Joardder, M. U. H., & Karim, M. A. (2016). Determination of appropriate effective diffusivity for different food materials. *Drying Technology, 35*(3), 335–346.
Kosasih, E. A., Zikri, A., & Dzaky, M. I. (2020). Effects of drying temperature, airflow, and cut segment on drying rate and activation energy of elephant cassava. *Case Studies in Thermal Engineering, 19*, Article 100633.
Lao, Y., Zhang, M., Sakamon, D., & Ye, Y. (2019). Effect of Combined infrared freeze drying and Microwave vacuum drying on quality of Kale Yoghurt Melts. *Drying Technology, 38*, 621–633.
Li, Y., Li, Y., Li, H., Qi, Y., Wu, Z., & Yang, M. (2017). Comparative study of microwave-vacuum and vacuum drying on the physicochemical properties and antioxidant capacity of licorice extract powder. *Powder Technology, 320*, 540–545.
Liu, Z., Xie, L., Zielinska, M., Pan, Z., Wang, J., Deng, L., et al. (2021). Pulsed vacuum drying enhances drying of blueberry by altering micro-, ultrastructure and water status and distribution. *LWT, 142*, Article 111013.
Li, L., Zhang, M., & Yang, P. (2019). Suitability of LF-NMR to analysis water state and predict dielectric properties of Chinese Yam during microwave vacuum drying. *LWT–Food Science and Technology, 105*, 257–264.
Mahdi Jafari, S., Ghalegi Ghalenoei, M., & Dehnad, D. (2017). Influence of spray drying on water solubility index, apparent density, and anthocyanin content of pomegranate juice powder. *Powder Technology, 311*, 59–65.
Mbegbu, N. N., Nwajinka, C. O., & Amaefule, D. O. (2021). Thin layer drying models and characteristics of scent leaves (Ocimum gratissimum) and lemon basil leaves (*Ocimum africanum*). *Heliyon, 7*(1), Article e05945.
Michalska, A., Wojdyło, A., Lech, K., Lysiak, G. P., & Figiel, A. (2016). Physicochemical properties of whole fruit plum powders obtained using different drying technologies. *Food Chemistry, 207*, 223–232.
Ming, L. J., & Yin, A. C. Y. (2013). Therapeutic effects of glycyrrhizic acid. *Natural Product Communications, 8*(3), 415–418.
Qiu, S., Bai, M., Zhao, P., Liu, Z., Huang, X., & Song, S. (2021). Phytochemical and network-based chemotaxonomic study of *Lonicera japonica* Thunb. *Biochemical Systematics and Ecology, 94*, Article 104210.
Rahman, A., & Chul Kang, C. (2009). In vitro control of food-borne and food spoilage bacteria by essential oil and ethanol extracts of Lonicera japonica Thunb. *Food Chemistry, 116*, 670–675.
Santhalakshmy, S., John Don Bosco, S., Francis, S., & Sabeena, M. (2015). Effect of inlet temperature on physicochemical properties of spray-dried jamun fruit juice powder. *Powder Technology, 274*, 37–43.
Sehrawat, R., Nema, P. K., & Kaur, B. P. (2018). Quality evaluation and drying characteristics of mango cubes dried using low-pressure superheated steam, vacuum and hot air drying methods. *LWT - Food Science and Technology, 92*, 548–555.
Sridhar, K., & Linton Charles, A. (2019). In vitro antioxidant activity of Kyoho grape extracts in DPPH and ABTS assays: Estimation methods for EC50 using advanced statistical programs. *Food Chemistry, 275*, 41–49.
Sun, Q., Zhang, M., & Yang, P. Q. (2019). Combination of LF-NMR and BP-ANN to monitor water states of typical fruits and vegetables during microwave vacuum drying. *LWT - Food Science and Technology, 116*, Article 108548.
Tanaka, T., Miyazaki, K., & Yabuki, T. (2020). Electrolytic bubble nucleation activation in pool boiling of water: Heat transfer enhancement and reduction of incipient boiling superheat. *International Journal of Heat and Mass Transfer, 157*, Article 119755.
Tan, S. P., Kha, T. C., Parks, S. E., Stathopoulos, C. E., & Roach, P. D. (2015). Effects of the spray-drying temperatures on the physiochemical properties of an encapsulated bitter melon aqueous extract powder. *Powder Technology, 281*, 65–75.
Vega-Gálvez, A., Ah-Hen, K., Chacana, M., Vergara, J., Martínez-Monzó, J., García-Segovia, P., et al. (2012). Effect of temperature and air velocity on drying kinetics, antioxidant capacity, total phenolic content, colour, texture and microstructure of apple (var. *Granny Smith*) slices. *Food Chemistry, 132*(1), 51–59.
Wang, H., Karim, M. A., Vidyarthi, S. K., Xie, L., Liu, Z. L., Gao, L., et al. (2021). Vacuum-steam pulsed blanching (VSPB) softens texture and enhances drying rate of carrot by altering cellular structure, pectin polysaccharides and water state. *Innovative Food Science & Emerging Technologies, 74*, Article 102801.
Wang, H., Li, X., Wang, J., Vidyarthi, S. K., Wang, H., Zhang, X. G., et al. (2022). Effects of postharvest ripening on water status and distribution, drying characteristics, volatile profiles, phytochemical contents, antioxidant capacity and microstructure of kiwifruit (Actinidia deliciosa). *Food Control, 139*, Article 109062.
Xiao, M., Tian, J., Zhou, Y., Xu, X., Min, X., Lv, Y., et al. (2020). Efficacy of Huoxiang Zhengqi dropping pills and Lianhua Qingwen granules in treatment of COVID-19: A randomized controlled trial. *Pharmacological Research, 161*, Article 105126.
Xu, P., Peng, X., Yang, J., Li, X., Zhang, H., Jia, X., et al. (2021). Effect of vacuum drying and pulsed vacuum drying on drying kinetics and quality of bitter orange (*Citrus aurantium L.*) slices. *Journal of Food Processing and Preservation, 45*(12), Article e16098.
Xu, P., Peng, X., Yuan, T., Yang, J., Li, X., Zhang, H., et al. (2021). Effect of vacuum drying on drying kinetics and quality of the aqueous extracts of *Callicarpa nudiflora* Hook. et Arn. *LWT–Food Science and Technology, 152*, Article 112305.
Yang, X., Han, Z., Xia, T., Xu, Y., & Wu, Z. (2021). Monitoring the oxidation state evolution of unsaturated fatty acids in four microwave-treated edible oils by low-field nuclear magnetic resonance and 1H nuclear magnetic resonance. *LWT - Food Science and Technology, 138*, Article 110740.
Yang, B., Zhong, Z., Wang, T., Ou, Y., Tian, J., Komatsu, S., et al. (2019). Integrative omics of Lonicera japonica Thunb. Flower development unravels molecular changes regulating secondary metabolites. *Journal of Proteomics, 208*, Article 103470.
Zhao, D., Wei, J., Hao, J., Han, X., Ding, S., Yang, L., et al. (2019). Effect of sodium carbonate solution pretreatment on drying kinetics, antioxidant capacity changes, and final quality of wolfberry (Lycium barbarum) during drying. *LWT - Food Science and Technology, 99*, 254–261.